

SEAR: A Polynomial-Time Expected Constant-Factor Optimal Algorithmic Framework for Multi-Robot Path Planning

Shuai D. Han Edgar J. Rodriguez Jingjin Yu

Abstract—This work studies the labeled multi-robot path and motion planning problem in continuous domains, in the absence of static obstacles. Given n robots which may be arbitrarily close to each other and assuming random start and goal configurations for the robots, we derived an $O(n^3)$, complete algorithm that produces solutions with constant-factor optimality guarantees on both makespan and distance optimality, in expectation. Furthermore, our algorithm only requires a small constant factor expansion of the initial and goal configuration footprints for solving the problem. In addition to strong theoretical guarantees, we present a thorough computational evaluation of the proposed solution. Beyond the baseline solution, adapting an effective (but non-polynomial time) robot routing subroutine, we also provide a highly efficient implementation that quickly computes near-optimal solutions. Hardware experiments on microMVP platform composed of non-holonomic robots confirms the practical applicability of our algorithmic pipeline.

I. INTRODUCTION

In a labeled multi-robot path planning (MPP) problem¹, the task is to move a set of rigid bodies (e.g., vehicles, mobile robots, quadcopters) from an initial configuration to a goal configuration in a collision-free manner. As a key sub-problem that needs to be solved in many multi-robot systems, fast, optimal, and practical resolution to MPP are actively sought after in both academic research and industrial applications. On the other hand, MPP, in its many forms, have been shown to be computationally hard [1]–[4]. Given the high computational complexity of MPP, there has been a lack of complete algorithms that provide concurrent guarantees on computational efficiency and solution optimality.

In this paper, we take initial steps to fill this long-standing optimality-efficiency gap in labeled multi-robot path planning in *continuous domains*, without the presence of static obstacles. We denote this version of the MPP problem as CMPP. Through a shift-expand-assign-route (SEAR) solution pipeline and the adaptation of a proper discrete robot routing algorithm [5], we derive a first polynomial time algorithm for solving CMPP in arbitrary dimensions that guarantees constant-factor solution optimality on both makespan and total distance, in expectation. For both start

S. D. Han and J. Yu are with the Department of Computer Science, Rutgers, the State University of New Jersey, Piscataway, NJ, USA. {shuai.han, jingjin.yu}@rutgers.edu. E. J. Rodriguez is with the Department of Mathematics, University of California Berkeley, Berkeley, CA, USA. ejaramillo@berkeley.edu.

¹In this paper, path planning and motion planning carry identical meanings, i.e., the computation of time-parametrized, collision-free, dynamically feasible solution trajectories. We often use MPP as an umbrella term to refer to multi-robot path (and motion) planning problems.

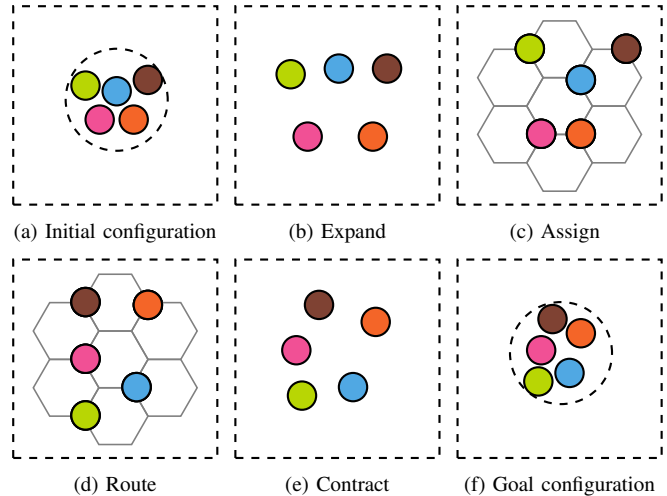


Fig. 1. Illustration of the expand-assign-route part of the (SEAR) pipeline. (a) the initial configuration. (a)→(b) expansion to create space for moving the robots around. (b)→(c) matching and snapping the robots onto a grid structure. (c)→(d) routing the robots on graphs. (d)→(e)→(f) the contraction step, which is the reverse of the expand-assign steps. (f) the goal configuration.

and goal configurations, the robots may be located arbitrarily close to each other.

This work brings forth two main contributions. The first and key contribution is the introduction of the SEAR pipeline as a general framework for solving CMPP in an obstacle-free but densely packed setting. With a proper discrete routing algorithm, we show that SEAR comes with strong theoretical guarantees on both computational time and solution optimality, which significantly improves over the state-of-the-art, e.g., [6]. Secondly, we have developed practical open source implementations² of multiple SEAR-based algorithms, including ones that use fast (but non-polynomial time) discrete routing subroutines. As demonstrated through extensive simulation studies, SEAR can readily tackle problem instances with a thousand densely packed robots. We further demonstrate that SEAR supports certain differential constraints with hardware experiments.

Related work. Variations of the multi-robot path planning problem have been actively studied for decades [7]–[17]. MPP finds applications in a diverse array of areas including assembly [18], evacuation [19], formation [20]–[22], localization [23], microdroplet manipulation [24], object transportation [25], [26], search and rescue [27], and human robot interaction [28], to list a few. Methods for resolving MPP can

²The source code associated with the current work will be added to our existing open source contributions upon the publication of the work.

be *centralized*, where a central planner dictates the motion of all moving robots, or *decentralized*, where the moving robots make individual decisions [10], [29], [30]. Given the focus of the paper, our review of related literature focuses on centralized methods.

In a centralized planner, with full access to the global system state, global planning and control can be readily enforced to drive operational efficiency. Methods in this domain may be further classified as *coupled*, *decoupled*, or a mixture of the two. *Coupled methods* treat all robots as a *composite* robot residing in $\mathcal{C} = \mathcal{C}^1 \times \dots \times \mathcal{C}^n$, where \mathcal{C}^i is the configuration space of a single robot [31] and subsequently the problem is subjected to standard single robot planning methods [32], [33], such as A* in discrete domains [34] and sampling-based methods in continuous domains [35]. However, similar to high dimensional single robot problems [36], MPP is strongly NP-hard for discs in simple polygons [1] and PSPACE-hard for translating rectangles [2]. The hardness of the problem extends to the unlabeled case [3] although complete and optimal algorithms for practical scenarios have been developed [13], [37]–[39].

In contrast, *decoupled methods* approach the problem by first computing a path for each individual robot while ignoring all other robots. Interactions between paths are only considered *a posteriori*. The delayed coupling allows more robots to be simultaneously considered but may induce the loss of completeness [40]. One can however achieve completeness using optimal decoupling [41]. The classical approach in decoupling is through *prioritization*, in which an order is forced upon the robots [7], potentially significantly affect the solution quality [42], though remedy is possible to some extent [43]. Sometimes the priority may be imposed on the fly, which involves plan-merging and deadlock detection [44]–[46]. Often, priority is used in conjunction with *velocity tuning*, which iteratively decides the velocity of lower priority robots [47]. Support for systems with differential constraints has also been added [48].

In the past decade, significant progress has been made on *optimally* solving (labeled) MPP problems in discrete settings, in particular on discrete (graph-base) environments. Here, the feasibility problem is solvable in $O(|V|^3)$ time, in which $|V|$ is the number of vertices of the graph on which the robots reside [49]–[51]. Optimal MPP remains computationally intractable in a graph-theoretic setting [4], [52], but the complexity has dropped from PSPACE-hard to NP-complete in many cases. On the algorithmic side, decoupling-based heuristics continue to prove to be useful [11], [15], [53]. Beyond decoupling, other ideas have also been explored, often through reduction to other problems [54]–[56].

Organization. The rest of this paper is structured as follows. In Section II, we formally state the problem studied in this paper. In Section III, with the establishment of the lower bound on achievable solution optimality, we introduce the SEAR pipeline at a high level. In Section IV, we describe the SEAR framework in full detail and provide theoretical analysis of its key properties. In Section V, we evaluate

the performance of algorithms explained in this paper. We conclude the paper in Section VI.

II. PROBLEM FORMULATION

Consider an obstacle-free k dimensional environment ($k \geq 2$) and a set of n labeled spherical (discs for 2D) robots $\mathcal{R} = \{1, \dots, n\}$ with a homogenous radius r . The robots move with speed $\|v\| \in [0, 1]$. The setup yields a configuration space $\mathcal{C} = \mathbb{R}^{kn}$; a configuration $X(t) \in \mathcal{C}$ is an injective map $X(t) : \mathcal{R} \rightarrow \mathbb{R}^{kn}$, which specifies the center of each robot at time t . Let $x_i(t)$ denote the location of robot i , i.e., $X(t) = \{x_1(t), \dots, x_n(t)\}$. Let $\|x_i(t)x_j(t)\|$ denote the Euclidean distance between $x_i(t)$ and $x_j(t)$. For collision avoidance, we require that

$$\forall 1 \leq i < j \leq n, t \in \mathbb{R}_{\geq 0}, \|x_i(t)x_j(t)\| > 2r,$$

where $\mathbb{R}_{\geq 0}$ is the set of all non-negative real numbers. We denote the initial and goal configurations as X^I and X^G , respectively, so that each robot i is assigned an initial location x_i^I and a goal location x_i^G . The continuous MPP instance studied in this paper may be defined as follows.

Problem 1 (Continuous Multi-Robot Path Planning (CMPP)). *Given (\mathcal{R}, X^I, X^G) , find a continuous plan $X(t) : [0, T] \rightarrow \mathcal{C}$ with $X(0) = X^I$ and $X(T) = X^G$.*

For the CMPP formulation, we would like to find solutions with optimality assurance, according to the following objectives:

- 1) **Min-Makespan.** Minimizing the required time to finish the task, i.e. T .
- 2) **Min-Total-Distance.** Minimizing the cumulative distance traveled by all robots.

In particular, we are interested in situations where X^I and X^G are very dense, i.e., the robots may assume configurations that leave them almost contacting each other.

For deriving and stating analytical results, we introduce some additional notations. For simplicity, we henceforth limit the discussion to two dimensional workspaces, i.e., $k = 2$. However, our results fully generalize to arbitrary fixed dimensions. Given X^I (resp., X^G), let c^I (resp., c^G) centered at o^I (resp., o^G) be the smallest bounding circle that encloses all n robots. I.e., let the radius of c^I (resp., c^G) be r^I (resp., r^G), then for all $1 \leq i \leq n$, $\|o^I x_i^I\| \leq r^I - r$ (resp., $\|o^G x_i^G\| \leq r^G - r$). Let $r_b = \max\{r^I, r^G\}$ and let $d = \|o^I o^G\|$ be the distance between the centers of the bounding circles. r_b and d will be used in stating our optimality results. An illustrative CMPP instance with these additional parameters is given in Fig. 2.

We note that the derivation of the constant-factor optimality lower bound requires an additional (mild) assumption that within the initial and goal configuration, x^I and x^G , the distribution of robot labels is uniformly random.

III. MAIN RESULTS

In this section, we outline the main algorithmic and analytical results of the paper: the SEAR pipeline and its constant-factor optimality guarantee for solving CMPP.

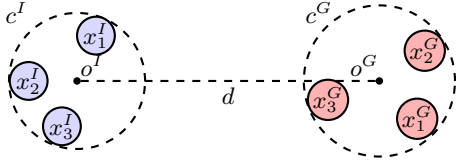


Fig. 2. Illustration of CMPP when $n = 3$ and $k = 2$. The large circles are the bounding circles c^I and c^G with radii r^I and r^G , respectively. In this case, $r_b = r^G$. The blue and red shaded discs show the locations of the robots.

A. Lower Bound on CMPP

We first establish a straightforward lower bound on the achievable optimality for CMPP under the assumption that X^I and X^G are randomly distributed.

Lemma III.1. *For obstacle-free CMPP with randomly distributed X^I and X^G , the lower bound of makespan is $\Omega(r_b + d)$ and the lower bound of total travel distance is $\Omega(n(r_b + d))$, in expectation.*

Proof. Consider a single robot j and the case where $o^I = o^G$, i.e., $d = 0$. In this case, in expectation, $\|x_j^I o^I\| = \Theta(r^I)$ and $\|x_j^G o^G\| = \Theta(r^G)$. With at least probability $1/2$, $\|x_j^I o^I\| < \|x_j^I x_j^G\|$ and $\|x_j^G o^G\| < \|x_j^I x_j^G\|$. Therefore, in expectation, $\|x_j^I x_j^G\| = \Omega(\max\{r^I, r^G\}) = \Omega(r_b)$. Using a similar argument, for $d > 0$, we have that $\|x_j^I x_j^G\| = \Omega(r_b + d)$ in expectation. This directly yields the desired makespan bound. The total distance bound follows by linearity of expectation. \square

B. SEAR and the Upper Bound on CMPP

The high-level pseudocode of SEAR, as partially illustrated in Fig. 1, is outlined in Alg. 1. The SEAR pipeline contains four essential steps: (i) shift, (ii) expand, (iii) assign, and (iv) route. At the start of the pseudo code (Line 1), the *shift* step moves the robots from X^I , without changing their relative positions so the centers of the bounding circles c^I and c^G coincide. Then, Lines 2-4, which correspond to the *expand* and *assign* steps, do the following: (i) expand the robots so that they are sufficiently apart, (ii) generate an underline grid $G(V, E)$, and (iii) perform an injective assignment from $\mathcal{R} \rightarrow V$. This then yields a MPP sub-problem in discrete domain. Line 5 solves the new MPP problem. Line 6 then reverse the expand-assign to reach X^G . Note that the sub-plan for the *contract* step is actually generated together with the expand and assign steps. In particular, only a single grid G is created. Because of this, we do not include this as a unique step of the SEAR pipeline.

Algorithm 1: SEAR Pipeline

- 1 **Shift:** move all robots so o^I overlaps o^G
 - 2 **Expand:** increase clearance between the robots
 - 3 $G(V, E) \leftarrow$ Construct a grid graph
 - 4 **Assign:** assign \mathcal{R} to V
 - 5 **Route:** solve the generated MPP on G
 - 6 **Contract:** reverse of expand-assign steps
-

We briefly analyze the optimality guarantee provided by SEAR; the details will follow in the next section. For an

arbitrary robot, the shift step brings a distance cost of d . The expand step incurs a cost of $O(r^I) \subseteq O(r_b)$ and the assign step a cost of $O(r)$. This suggests that the contract step also incurs a cost of $O(r_b + r) = O(r_b)$. The route step, using [5], incurs a cost of $O(r_b)$ as well. Adding everything together, for a single robot, the total distance that is traveled is $O(d + r_b)$. Since the SEAR pipeline solve the problem for all robots simultaneously, the makespan is $O(d + r_b)$ and the total distance traveled is $O(n(d + r_b))$. In viewing Lemma III.1, we summarize the section with the following theorem, to be proved shortly.

Theorem III.1. *For obstacle-free CMPP with randomly distributed X^I and X^G , an SEAR-based algorithm can compute constant-factor optimal solutions for makespan and total traveled distance, in expectation.*

IV. THE SEAR PIPELINE

In this section, we present the details of SEAR, supported with full analysis.

A. Shift

According to Lemma III.1, when $d > 0$, the expected optimality lower bound for each robot is $\Omega(d + r_b)$ regardless of time and distance. This suggests that if our algorithm solves part of the problem with optimality $O(d)$, it will not break the constant factor guarantee. Seeing this, the SEAR pipeline starts with a shift step that translates the robots from X^I so o^I is moved to o^G without changing the relative positions of the robots (see Fig. 3). Because of the assumption that the workspace is free of static obstacles, this can always be readily achieved. This yields a new CMPP problem with $d = 0$. This process incurs exactly d makespan and nd total travel distance. The computational complexity is $O(n)$ because we need to plan trajectories for n robots, and for each of them, the path is just simply a straight line that starts from x_i^I and follows the vector $o^I o^G$.

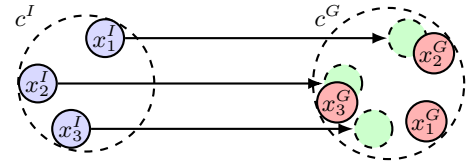


Fig. 3. For the scenario illustrated in Fig. 2, we may shift the robots so that o^I is moved to o^G .

Without loss of generality, in the remaining part of this section, we assume $o^I = o^G$, and $d = 0$ in a CMPP instance, unless otherwise stated.

B. Expand and Assign

The purpose of *expand* and *assign* is to convert CMPP into MPP, i.e., a continuous problem into a discrete one. To achieve this, we apply expand and assign routines to both X^I and X^G . As a brief explanation, a regular grid graph $G = (V, E)$ is first created based on r , the size of the robots. The goal is to move the robots from (potentially shifted) X^I and X^G onto vertices of G . The process for doing this for

X^I and X^G are exactly the same; we use X^I to illustrate the routines.

1) *Expand*: The expand routine expands robots from X^I so that there are enough clearance between them for moving them onto the graph G . For doing so, we use simple *linear expansion* as defined below.

Definition IV.1. Linear Expansion. Each robot i moves along the direction of vector $\overrightarrow{o^I x_i^I}$ at the maximum speed 1. The total distance traveled by a robot i is $(\lambda - 1)\|o^I x_i^I\|$, where $\lambda \geq 1$ is a *scaling factor*.

The value of λ , to be decided later, depends on the grid type and also the smallest distance between a pair of robots in X^I . We now show that linear expansion is collision free.

Lemma IV.1. *Linear expansion is always collision-free.*

Proof. Because linear expansion with scaling factor λ applies different travel distances to robots, we need to eliminate potential collisions between two moving robots, as well as between one moving robot and another stopped robot.

As it is shown in Fig. 4(a), a pair of moving robots i and j always travel the same distance t during time $[0, t]$ because they both move at the maximum speed 1. Denote $a = \|o^I x_i^I\|, b = \|o^I x_j^I\|, \alpha = \angle x_i^I o^I x_j^I$. The increased distance between the center of i, j after linear expansion is

$$(a+t)^2 + (b+t)^2 - 2(a+t)(b+t)\cos\alpha - \|x_i^I x_j^I\| \\ = 2(1 - \cos\alpha)(ta + tb + t^2) \geq 0.$$

Since $\|x_i^I x_j^I\| > 2r$, two moving robots cannot collide.

The robots which are stopped earlier will not collide with any other robots afterwards. See Fig. 4(b), after robot 1 stopped moving, the robots closer to o^I (robot 2, 3, centered in the shaded area) are already stopped, and the other robots (robot 4, 5, 6, centered out of the shaded area) are moving towards outside, which cannot cause collisions with robot 1 in the future. \square

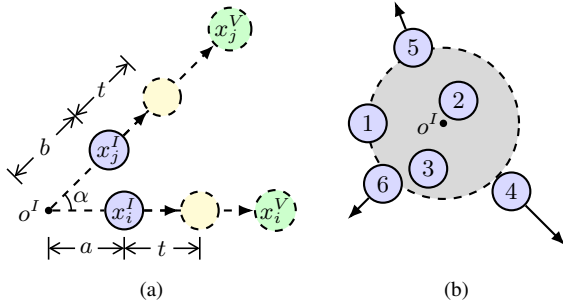


Fig. 4. Linear expansion. (a) Any two moving robots are collision-free. (b) The robots stopped will not collide to any other robots afterwards.

Corollary IV.1. *The distance between the center of any two robots after linear expansion is scaled up by a factor of λ .*

Proof. See Fig. 4(a), assume x_i^V, x_j^V are the location for robot i, j after linear expansion, respectively. Because $\lambda = \|o^I x_i^V\|/\|o^I x_i^I\| = \|o^I x_j^V\|/\|o^I x_j^I\|$, $\lambda = \|x_i^V x_j^V\|/\|x_i^I x_j^I\|$. \square

The makespan of linear expansion is $O(\lambda r_b)$, because the travel distance of any robot cannot exceed $(\lambda - 1)(r_b - r)$. For the same reason, the total travel distance is $O(n\lambda r_b)$.

Remark. Depending on the specific problem instance, expansion could be achieved through multiple ways, as long as the robots moves in a collision-free manner. That is, expand can be done in a smarter way. However (intuitively and as we will show), linear expansion with a small constant λ is sufficient for the SEAR analysis to carry through. Moreover, there cannot exist any method that do better than $\Omega(r_b)$.

2) *Assign*: After expansion, we generate a regular grid graph G in a rectangular area covering all the robots. Here, we use hexagonal grid for illustration due to its capability for accommodating high robot density and natural support for certain differential constraints [57]. In order to make the robots move along edges in such a grid graph G without collisions, the edge/side length ℓ should be at least $(4/\sqrt{3})r$ [57]. We first establish the number of vertices for a G that covers the expanded X^I .

Lemma IV.2. *The number of vertices in G is $O(\lambda^2 r_b^2 / \ell^2)$.*

Proof. After the linear expansion, the radius of the smallest circle contains all the robots is not larger than λr_b . If we construct G in this area, then $|V| = O(\lambda^2 r_b^2 / \ell^2)$. \square

After G is built, we plan the trajectories to place the robots on the vertices in G . This is done by assigning each robot to the nearest vertex, and execute the straight line path at full speed 1. We need to establish that this process is collision-free. For a given X^I , we define $d_{min} = \min_{1 \leq i < j \leq n} \|x_i^I x_j^I\|$.

Lemma IV.3. *If $\lambda \geq 2\ell/d_{min}$, the mapping between \mathcal{R} and V is injective and the assigned paths are collision-free.*

Proof. The assumption, combined with Corollary IV.1, implies that after the linear expansion, robots are located in non-overlapping circles with radius ℓ (see Fig. 5(a)). Since G is a hexagonal grid, there must be at least one vertex in G lands inside or on the border of each circle, which is assigned to the robot in this circle. This ensures the injective mapping between \mathcal{R} and V .

To prove the paths are collision-free, let i and j be a pair of robots for which $d_{min} = \|x_i^I x_j^I\|$ (Fig 5(b)). Suppose the center location of the robots after expansion are x_i^V, x_j^V , and v_i, v_j are the vertices assigned to the two robots, respectively. Then, if $\lambda \geq 2\ell/d_{min}$, we have

$$\|x_i^V v_i\| \leq \ell, \|v_i v_j\| \geq \ell, \|x_i^V v_j\| \geq \ell, \|x_i^V x_j^V\| \geq 2\ell.$$

This implies that the distance (the red dashed line) from v_j to segment $x_i^V v_i$ is at least $(\sqrt{3}/2)\ell$. The above statements also holds for v_i and $x_j^V v_j$. Thus, the shortest distance between paths $x_i^V v_i$ and $x_j^V v_j$ is $(\sqrt{3}/2)\ell \geq 2r$. No collisions between robot i, j . \square

If we let $\ell = (4/\sqrt{3})r$, Since $2\ell/d_{min} \leq \ell/r = 4/\sqrt{3}$, It is safe to say that when $\lambda = 4/\sqrt{3}$, the expand-assign can always be successfully performed. λ can be smaller when

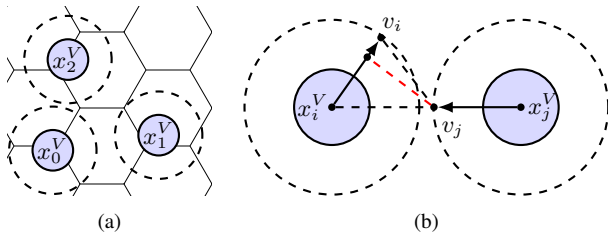


Fig. 5. Assign. (a) The robots are in circles with radius ℓ which do not overlap. (b) No collision between the paths.

d_{min} is larger. In any case, the makespan for the whole expand-assign step is $O(r_b)$, and the total travel distance is $O(nr_b)$. In viewing Lemma IV.2, the computational time is $O(n^2)$, with the dominating factor being matching the robots with their nearest vertices.

Other grids could also be used so long as there is no collision in the matching step. For example, the edge length of a grid graph with square cells should be at least $4/\sqrt{2}$. $\lambda = 2$ is sufficient for collision-free solutions in this case.

An alternative for the expand-assign step is to consider matching \mathcal{R} to V as an unlabeled MPP problem in continuous domain. Because the makespan for expand-assign is already sufficient for achieving the desired optimality, we opt to keep the method fast and straightforward.

Remark. In the actual implementation, we also added an extra step that “compacts” the MPP instance, which makes the start and goal configurations on the graph G more concentrated. The extra step, based largely on [37], does not impact the asymptotic performance of the SEAR pipeline but produces better constants.

C. Route

After applying expand and assign steps to both X^I and X^G , a CMPP instance becomes a (discrete) MPP instance. Let the converted instance be (G, V^I, V^G) , i.e., $V^I = \{v_1^I, \dots, v_n^I\}$ and $V^G = \{v_1^G, \dots, v_n^G\}$ are the discrete initial and goal configurations of the robots on the grid graph G . To solve the MPP instance with polynomial time complexity and optimality guarantee, we apply the SPLITANDGROUP (SAG) algorithm [5]. The algorithm is intended for a fully occupied graph, but is also directly applicable to sparse graphs: we may place “virtual robots” on empty vertices. For completeness, we provide a brief overview of SAG here.

SAG is a recursive algorithm that splits an MPP instance into smaller sub-problems in each level of the recursive call. Let us use one recursion as an example. As shown in Fig. 6(a), *split* partitions the part of grid it works on into two areas (left side with a blue shade and right side with a red shade) along the longer side of this grid. On each side, the algorithm finds all the robots i currently on this side with v_i^G on the other side. Here in Fig. 6, the blue (red) robots are the ones with goal vertices in blue (red) shade, respectively. Then during this recursive call, *group* moves every robot to the side where its goal vertex belongs to (see Fig. 6(b)). This results in two sub-problems (the left one and the right one), which could be treated by the next recursion call in parallel.

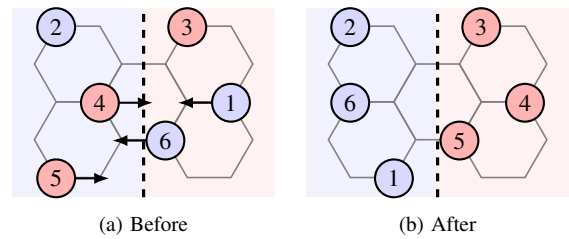


Fig. 6. Before and after one recursive call of SAG.

The grouping procedure depends on the robots being able “swap” locations locally in constant time. This is where the grid graph helps. On a hexagonal grid, swapping of locations for any two robots on a fully occupied *figure-8 graph* (Fig. 7) can be performed in constant time through an adaptation of the proof used in proving Lemma 1 of [5]. As a larger grid is partitioned into these smaller figure-8 graphs, parallel swaps become possible. Let G be bounded in a rectangle of size $m_w \times m_h$ in which m_w and m_h are the width and height of the rectangle, then the first iteration of SAG requires a robot incur a makespan of $O(m_w + m_h)$ and this can be done in parallel for all robots. Recursively, the makespan upper bound of SAG (applied to our problem) is:

$$\begin{aligned} & O(m_w + m_h) + O\left(\frac{m_w}{2} + m_h\right) + O\left(\frac{m_w}{2} + \frac{m_h}{2}\right) + \dots \\ & = O(m_w + m_h) = O(\lambda r_b) = O(r_b). \end{aligned}$$

The last equality is due to λ being small constant.



Fig. 7. A figure-8 graph.

SAG incurs $O(|V|^3) = O(n^3)$ computational time.

D. Performance Analysis of SEAR

Summarizing the result for the individual steps, for the general SEAR pipeline with the shift step, we conclude

Theorem IV.1. *For obstacle-free CMPP, SEAR computes solutions with $O(r_b + d)$ makespan and $O(n(r_b + d))$ total distance in polynomial time.*

Theorem III.1 follows Lemma III.1 and Theorem IV.1.

E. High Dimensions

We briefly discuss how the the SEAR pipeline readily generalized to higher dimensions. The proofs of the shift, expand, and assign steps of SEAR readily generalizes to arbitrary dimensions. Also, for any fixed dimension, the guarantee of the SAG algorithm continuous to hold [5].

V. EVALUATION

In this section, we provide evaluations of the computational time and solution optimality of SEAR-based algorithms. A hardware experiment is also carried out to verify support for differential constraints. In our implementation, beside the baseline SEAR with SAG, we also implemented an SEAR algorithm with the high quality (but non-polynomial-time) ILP solver from [56]. To differentiate

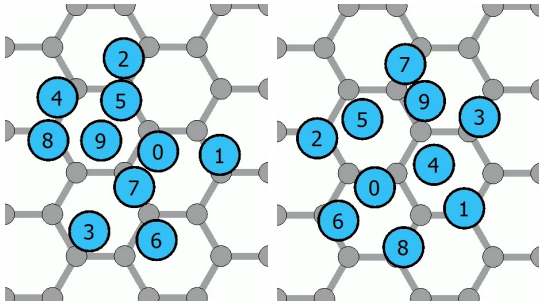


Fig. 8. An example of a randomly generated CMPP with $n = 10$, $\varepsilon = 0$, $d = 0$. The left and right figure indicates X^I and X^G , respectively. Part of the hexagonal graph generated by SEAR is rendered in the background.

the methods, we denote SEAR with SAG as SEAR-SAG, and SEAR with ILP solver as SEAR-ILP. SEAR-ILP- m indicates the usage of m -way split heuristics [56]. We use makespan as the key metric which also bounds the total distance and maximum distance. Additionally, instead of simply using the makespan value, which is less informative, we divide it by an underestimated minimum makespan, which is the maximum of the shortest distance between the start and goal pairs.

We implement SEAR-SAG in Python. The SEAR-ILP implementation is partially based on the Java code from [56], which utilizes the Gurobi ILP solver [58]. To capture denseness of the setup, we introduce a clearance parameter $\varepsilon = \min\{\min_{1 \leq i < j \leq n} \|x_i^I x_j^I\|, \min_{1 \leq i < j \leq n} \|x_i^G x_j^G\|\} - 2r$. Since the robot radius r is relative, we fix $r = 1$. In generating instances, the region where the robots may appear is limited to a circle of radius 1.5 times the radius of the smallest circle that n discs with radius $r + \varepsilon/2$ could fit in [59]. The edge length of hexagonal grids is $\ell = 4/\sqrt{3}$. The scaling factor $\lambda = \ell/(\varepsilon/2 + r)$. Our evaluation mainly focuses on the case of $d = 0$ since the shift step is straightforward. An example instance is provided in Fig. 8.

Instances for testing are generated with varied parameters. For each set of parameters, 10 randomly and sequentially generated instances are attempted and the average is taken. A data point is only recorded if all 10 instances are completed successfully. All experiments were executed on a Intel[®] Core[™] i7-6900K CPU with 32GB RAM at 2133MHz.

A. SEAR-SAG

To observe the basic behavior of SEAR-SAG, we fix $\varepsilon = d = 0$ and evaluate SEAR-SAG on both hexagonal grids and square grids by increasing n . For square grids, $l = 4/\sqrt{2}$, $\lambda = 2/(\varepsilon/2 + r)$. The result is in Fig. 9. From the computational time aspect (see Fig. 9 (a)), SEAR-SAG is able to solve problems with 1000 robots within hundreds of seconds. On the optimality side (see Fig. 9 (b)), because of the simple implementation and the sense setting, the optimality ratio of solutions generated by SEAR-SAG is relatively large. For example, the makespan for hexagonal grid is 75 times the underestimated makespan when $n = 20$. We can observed, however, that the ratio between the solution makespan and the underestimated makespan flattens out as n grows for both cases, confirming the constant factor

optimality property of SEAR.

We note that the guaranteed optimality of SEAR is in fact sub-linear with respect to the number of robots, which is clearly illustrated in Fig. 10. As we can observe, the makespan is proportional to the side length of the grid, which in turn is proportional to \sqrt{n} .

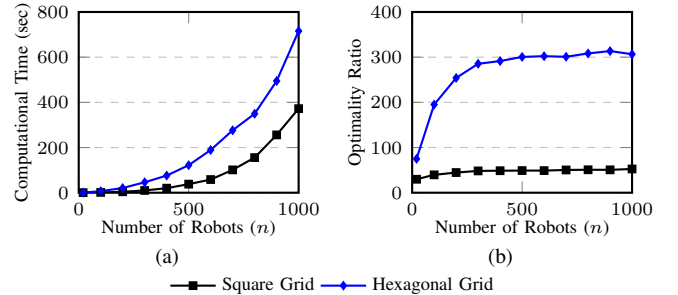


Fig. 9. Computational time and optimality ratio of SEAR-SAG versus the number of robots.

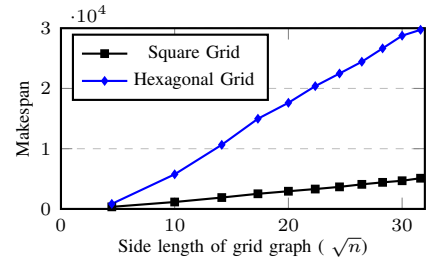


Fig. 10. Makespan of SEAR-SAG versus the number of vertices on the longer side of the grid.

B. SEAR-SAG vs. SEAR-ILP

We then compare SEAR-SAG and SEAR-ILP on hexagonal grids. First we let $\varepsilon = d = 0$ and gradually increase n . The performance of the algorithms agrees with the expectation (see Fig. 11). SEAR-ILP guarantees the optimal solution on the MPP sub-problem. However, its running time grows quickly and becomes unstable. It cannot always solve a problem instance in 30 minutes when $n > 50$. Nevertheless, the split heuristic makes SEAR-ILP more applicable when n is large. For example, the running time of SEAR-ILP with 4-way split is about the same as SEAR-SAG when $n = 700$. Although SEAR-ILP with split heuristic can solve problems with hundreds of robots, when $n \geq 800$, only SEAR-SAG could finish due to its polynomial time complexity.

The makespan of solutions generated by SEAR-ILP is quite low and practical, since it always provide the optimal solution to MPP sub-problems. For instance, when $n = 40$, the makespan of generated solutions is only 4.93 times the estimated value. The optimality of SEAR-ILP with split heuristics are also close to being optimal. When $n = 500$, SEAR-ILP with 4-way split provides solutions with makespan 4.73 times the underestimated value.

In order to model different density of robots, We then fix $n = 30$, $d = 0$ and increase ε . With a larger ε , λ could be smaller, which makes robots move less during linear scaling. Fig. 12 demonstrates the performance of the methods as ε goes from 0 to 2.6 (when $\varepsilon \geq 8/\sqrt{3} - 2 \approx 2.62$, no expansion

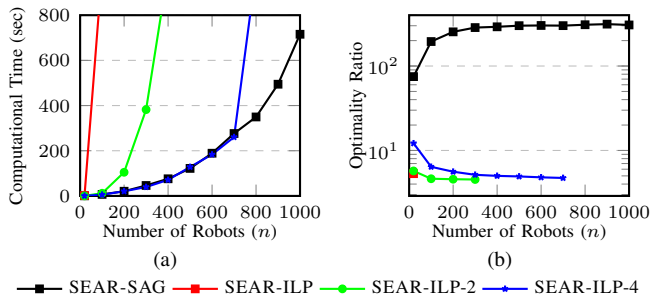


Fig. 11. Performance of SEAR algorithms as n varies.

is required). Here, since n and $|V|$ are not changed, the size of the MPP sub-problems remains the same. Thus the computational time of the algorithms stays static. On the other hand, the optimality ratio is lower when ε is large. This is because as the robots fall apart more, the expected makespan gets larger, while the makespan of the generated solution by SEAR does not change much.

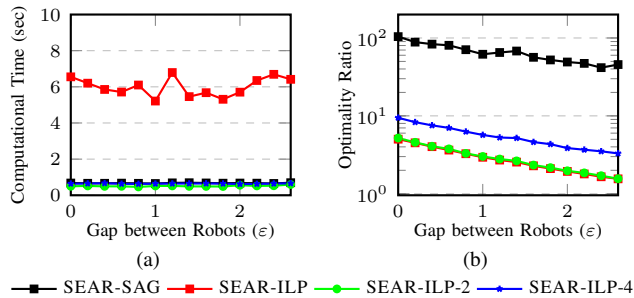


Fig. 12. Performance of SEAR algorithms as ε varies.

In the last part of our experiment, we fix $n = 30$, $\varepsilon = 0$ and change d . As we can observe in Fig.13, the solution becomes closer to optimal as d increases, as expected.

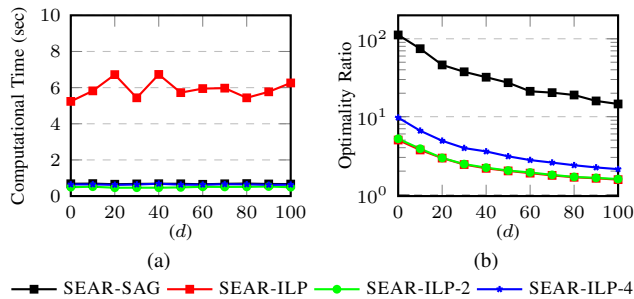


Fig. 13. Performance of SEAR algorithms as d varies.

Both the software simulation and hardware experimentation of the proposed algorithms can be found in the video attachment. The hardware implementation (details in Fig. 14) is based on the microMVP platform [60].

VI. CONCLUSION

In this paper, we proposed the SEAR solution pipeline for tackling continuous multi-robot path planning (CMPP) problem in the absence of static obstacles. We show that SEAR-based algorithms provide strong theoretical guarantees. With an alternative sub-routine for the discrete MPP instance, SEAR also proves to be practical, as confirmed by simulation and hardware experiment.

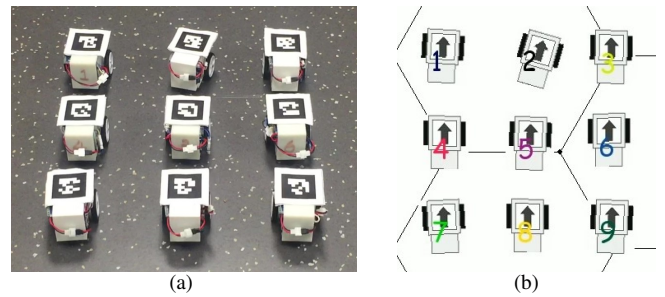


Fig. 14. The hardware experimentation. (a) The paths generated by SEAR are executed by differential drive cars. (b) Part of a Python-based UI, which is used to monitor and control the vehicles.

The current iteration of the SEAR-based algorithms has focused on theoretical guarantees; many additional improvements are possible. For example, the expand and assign steps can be done in an adaptive manner that avoids uniform scaling, which should greatly boost the optimality of the resulting algorithm. Additionally, the current SEAR pipeline only provide ad-hoc support for robots differential constraints. In an extension to the current work, we plan to further improve the efficiency and optimality of SEAR and add generic support for robots with differential constraints including aerial vehicle swarms.

REFERENCES

- [1] P. Spirakis and C. K. Yap, "Strong NP-hardness of moving many discs," *Information Processing Letters*, vol. 19, no. 1, pp. 55–59, 1984.
- [2] J. E. Hopcroft, J. T. Schwartz, and M. Sharir, "On the complexity of motion planning for multiple independent objects; PSPACE-hardness of the "warehouseman's problem",
" *The International Journal of Robotics Research*, vol. 3, no. 4, pp. 76–88, 1984.
- [3] K. Solovey and D. Halperin, "On the hardness of unlabeled multi-robot motion planning," in *Robotics: Science and Systems (RSS)*, 2015.
- [4] J. Yu, "Intractability of optimal multi-robot path planning on planar graphs," *IEEE Robotics and Automation Letters*, vol. 1, no. 1, pp. 33–40, 2016.
- [5] —, "Constant factor optimal multi-robot path planning in well-connected environments," *arXiv preprint arXiv:1706.07255*, 2017.
- [6] S. Tang and V. Kumar, "A complete algorithm for generating safe trajectories for multi-robot teams," in *Robotics Research*. Springer, 2018, pp. 599–616.
- [7] M. A. Erdmann and T. Lozano-Pérez, "On multiple moving objects," in *Proceedings IEEE International Conference on Robotics & Automation*, 1986, pp. 1419–1424.
- [8] S. M. LaValle and S. A. Hutchinson, "Optimal motion planning for multiple robots having independent goals," *IEEE Transactions on Robotics & Automation*, vol. 14, no. 6, pp. 912–925, Dec. 1998.
- [9] Y. Guo and L. E. Parker, "A distributed and optimal motion planning approach for multiple mobile robots," in *Proceedings IEEE International Conference on Robotics & Automation*, 2002, pp. 2612–2619.
- [10] J. van den Berg, M. C. Lin, and D. Manocha, "Reciprocal velocity obstacles for real-time multi-agent navigation," in *Proceedings IEEE International Conference on Robotics & Automation*, 2008, pp. 1928–1935.
- [11] T. Standley and R. Korf, "Complete algorithms for cooperative pathfinding problems," in *Proceedings International Joint Conference on Artificial Intelligence*, 2011, pp. 668–673.
- [12] K. Solovey and D. Halperin, " k -color multi-robot motion planning," in *Proceedings Workshop on Algorithmic Foundations of Robotics*, 2012.
- [13] M. Turpin, K. Mohta, N. Michael, and V. Kumar, "CAPT: Concurrent assignment and planning of trajectories for multiple robots," *International Journal of Robotics Research*, vol. 33, no. 1, pp. 98–112, 2014.
- [14] K. Solovey, J. Yu, O. Zamir, and D. Halperin, "Motion planning for unlabeled discs with optimality guarantees," in *Robotics: Science and Systems*, 2015.
- [15] G. Wagner and H. Choset, "Subdimensional expansion for multirobot path planning," *Artificial Intelligence*, vol. 219, pp. 1–24, 2015.

- [16] L. Cohen, T. Uras, T. Kumar, H. Xu, N. Ayanian, and S. Koenig, "Improved bounded-suboptimal multi-agent path finding solvers," in *International Joint Conference on Artificial Intelligence*, 2016.
- [17] B. Araki, J. Strang, S. Pohorecky, C. Qiu, T. Naegeli, and D. Rus, "Multi-robot path planning for a swarm of robots that can both fly and drive," in *IEEE Int. Conf. on Robotics and Automation (ICRA)*, 2017.
- [18] D. Halperin, J.-C. Latombe, and R. Wilson, "A general framework for assembly planning: The motion space approach," *Algorithmica*, vol. 26, no. 3-4, pp. 577-601, 2000.
- [19] S. Rodriguez and N. M. Amato, "Behavior-based evacuation planning," in *Proceedings IEEE International Conference on Robotics & Automation*, 2010, pp. 350-355.
- [20] S. Poduri and G. S. Sukhatme, "Constrained coverage for mobile sensor networks," in *Proceedings IEEE International Conference on Robotics & Automation*, 2004.
- [21] B. Shucker, T. Murphey, and J. K. Bennett, "Switching rules for decentralized control with simple control laws," in *American Control Conference*, Jul 2007, pp. 1485-1492.
- [22] B. Smith, M. Egerstedt, and A. Howard, "Automatic generation of persistent formations for multi-agent networks under range constraints," *ACM/Springer Mobile Networks and Applications Journal*, vol. 14, no. 3, pp. 322-335, Jun. 2009.
- [23] D. Fox, W. Burgard, H. Kruppa, and S. Thrun, "A probabilistic approach to collaborative multi-robot localization," *Autonomous Robots*, vol. 8, no. 3, pp. 325-344, Jun. 2000.
- [24] E. J. Griffith and S. Akella, "Coordinating multiple droplets in planar array digital microfluidic systems," *International Journal of Robotics Research*, vol. 24, no. 11, pp. 933-949, 2005.
- [25] M. J. Mataric, M. Nilsson, and K. T. Simsarian, "Cooperative multi-robot box pushing," in *Proceedings IEEE/RSJ International Conference on Intelligent Robots & Systems*, 1995, pp. 556-561.
- [26] D. Rus, B. Donald, and J. Jennings, "Moving furniture with teams of autonomous robots," in *Proceedings IEEE/RSJ International Conference on Intelligent Robots & Systems*, 1995, pp. 235-242.
- [27] J. S. Jennings, G. Whelan, and W. F. Evans, "Cooperative search and rescue with a team of mobile robots," in *Proceedings IEEE International Conference on Robotics & Automation*, 1997.
- [28] R. A. Knepper and D. Rus, "Pedestrian-inspired sampling-based multi-robot collision avoidance," in *2012 IEEE RO-MAN: The 21st IEEE International Symposium on Robot and Human Interactive Communication*. IEEE, 2012, pp. 94-100.
- [29] J. Snape, J. van den Berg, S. J. Guy, and D. Manocha, "The hybrid reciprocal velocity obstacle," *IEEE Transactions on Robotics*, vol. 27, no. 4, pp. 696-706, 2011.
- [30] S. Kim, S. J. Guy, K. Hillesland, B. Zafar, A. A.-A. Gutub, and D. Manocha, "Velocity-based modeling of physical interactions in dense crowds," *The Visual Computer*, vol. 31, no. 5, pp. 541-555, 2015.
- [31] J. T. Schwartz and M. Sharir, "On the piano movers problem. ii. general techniques for computing topological properties of real algebraic manifolds," *Advances in applied Mathematics*, vol. 4, no. 3, pp. 298-351, 1983.
- [32] J.-C. Latombe, *Robot motion planning*. Springer Science & Business Media, 2012, vol. 124.
- [33] S. M. LaValle, *Planning Algorithms*. Cambridge, U.K.: Cambridge University Press, 2006, also available at <http://planning.cs.uiuc.edu/>.
- [34] P. Hart, N. J. Nilsson, and B. Raphael, "A formal basis for the heuristic determination of minimum cost paths," *IEEE Transactions on Systems Science and Cybernetics*, vol. 4, pp. 100-107, 1968.
- [35] K. Solovey, O. Salzman, and D. Halperin, "Finding a needle in an exponential haystack: Discrete RRT for exploration of implicit roadmaps in multi-robot motion planning," in *Proceedings Workshop on Algorithmic Foundations of Robotics*, 2014.
- [36] J. H. Reif, "Complexity of the generalized mover's problem." DTIC Document, Tech. Rep., 1985.
- [37] J. Yu and S. M. LaValle, "Distance optimal formation control on graphs with a tight convergence time guarantee," in *Proceedings IEEE Conference on Decision & Control*, 2012, pp. 4023-4028.
- [38] A. Adler, M. De Berg, D. Halperin, and K. Solovey, "Efficient multi-robot motion planning for unlabeled discs in simple polygons," in *Algorithmic Foundations of Robotics XI*. Springer, 2015, pp. 1-17.
- [39] K. Solovey, J. Yu, O. Zamir, and D. Halperin, "Motion planning for unlabeled discs with optimality guarantees," *arXiv preprint arXiv:1504.05218*, 2015.
- [40] G. Sanchez and J.-C. Latombe, "Using a prm planner to compare centralized and decoupled planning for multi-robot systems," in *Robotics and Automation, 2002. Proceedings. ICRA'02. IEEE International Conference on*, vol. 2. IEEE, 2002, pp. 2112-2119.
- [41] J. van den Berg, J. Snoeyink, M. Lin, and D. Manocha, "Centralized path planning for multiple robots: Optimal decoupling into sequential plans," in *Robotics: Science and Systems*, 2009.
- [42] J. van den Berg and M. Overmars, "Prioritized motion planning for multiple robots," in *Proceedings IEEE/RSJ International Conference on Intelligent Robots & Systems*, 2005.
- [43] M. Bennewitz, W. Burgard, and S. Thrun, "Finding and optimizing solvable priority schemes for decoupled path planning techniques for teams of mobile robots," *Robotics and autonomous systems*, vol. 41, no. 2, pp. 89-99, 2002.
- [44] R. Alami, F. Robert, F. Ingrand, and S. Suzuki, "Multi-robot cooperation through incremental plan-merging," in *Robotics and Automation, 1995. Proceedings., 1995 IEEE International Conference on*, vol. 3. IEEE, 1995, pp. 2573-2579.
- [45] S. Qutub, R. Alami, and F. Ingrand, "How to solve deadlock situations within the plan-merging paradigm for multi-robot cooperation," in *Intelligent Robots and Systems, 1997. IROS'97., Proceedings of the 1997 IEEE/RSJ International Conference on*, vol. 3. IEEE, 1997, pp. 1610-1615.
- [46] M. Saha and P. Ito, "Multi-robot motion planning by incremental coordination," in *2006 IEEE/RSJ International Conference on Intelligent Robots and Systems*. IEEE, 2006, pp. 5960-5963.
- [47] K. Kant and S. Zucker, "Towards efficient trajectory planning: The path velocity decomposition," *International Journal of Robotics Research*, vol. 5, no. 3, pp. 72-89, 1986.
- [48] J. Peng and S. Akella, "Coordinating multiple robots with kinodynamic constraints along specified paths," in *Algorithmic Foundations of Robotics V*, J.-D. Boissonat, J. Burdick, K. Goldberg, and S. Hutchinson, Eds. Berlin: Springer-Verlag, 2002, pp. 221-237.
- [49] V. Auletta, A. Monti, M. Parente, and P. Persiano, "A linear-time algorithm for the feasibility of pebble motion on trees," *Algorithmica*, vol. 23, pp. 223-245, 1999.
- [50] G. Goral and R. Hassin, "Multi-color pebble motion on graph," *Algorithmica*, vol. 58, pp. 610-636, 2010.
- [51] J. Yu, "A linear time algorithm for the feasibility of pebble motion on graphs," *arXiv:1301.2342*, 2013.
- [52] O. Goldreich, "Finding the shortest move-sequence in the graph-generalized 15-puzzle is NP-hard," 1984, laboratory for Computer Science, Massachusetts Institute of Technology, Unpublished manuscript.
- [53] E. Boyarski, A. Felner, R. Stern, G. Sharon, O. Betzalel, D. Tolpin, and E. Shimony, "Icbs: The improved conflict-based search algorithm for multi-agent pathfinding," in *Eighth Annual Symposium on Combinatorial Search*, 2015.
- [54] P. Surynek, "Towards optimal cooperative path planning in hard setups through satisfiability solving," in *Proceedings 12th Pacific Rim International Conference on Artificial Intelligence*, 2012.
- [55] E. Erdem, D. G. Kisa, U. Öztok, and P. Schueller, "A general formal framework for pathfinding problems with multiple agents," in *AAAI*, 2013.
- [56] J. Yu and S. M. LaValle, "Optimal multi-robot path planning on graphs: Complete algorithms and effective heuristics," *IEEE Transactions on Robotics*, vol. 32, no. 5, pp. 1163-1177, 2016.
- [57] J. Yu and D. Rus, "An effective algorithmic framework for near optimal multi-robot path planning," in *Robotics Research*. Springer, 2018, pp. 495-511.
- [58] Gurobi Optimization, Inc., "Gurobi optimizer reference manual," 2014. [Online]. Available: <http://www.gurobi.com>
- [59] E. Specht, *The best known packings of equal circles in a circle (complete up to N = 2600)*, Nov. 2016. [Online]. Available: <http://hydra.nat.uni-magdeburg.de/packing/cci/cci.html>
- [60] J. Yu, S. D. Han, W. N. Tang, and D. Rus, "A portable, 3D-printing enabled multi-vehicle platform for robotics research and education," in *IEEE International Conference on Robotics and Automation*, 2017.